

MPM validation with centrifuge tests: pilot case pile installation

Part 1

dr. A.S.K. Elkadi
P. Nguyen Msc

1206750-005

Title
MPM validation with centrifuge tests: pilot case pile installation

Project 1206750-005	Reference 1206750-005-HYE-0001- jvm	Pages 31
-------------------------------	--	--------------------

Keywords
Material Point Method (MPM), pile installation, Mohr-Coulomb





Summary
Numerical calculations using the dynamic MPM-code of Deltares are performed to simulate the modelling of installation effects of piles. Aim of the project is the validation of the numerical calculations using results of centrifuge tests, which were carried out at Deltares. The centrifuge tests were performed to analyse the installation effects of jacked piles and for the simulation of static and rapid load tests, see Huy (2008). This is follow-up of the work "On the validation of the Material Point Method (MPM)" reported by Rohe et.al, 2013.

Aim of the numerical simulations is to model the pile installation effects to create the load-displacement behaviour resulting from the installation. After the simulation of the installation phase the loading scheme has to be applied which corresponds to the static load test as used in the centrifuge experiment.

The work is divided into two phases; first phase, which is reported here, is the analysis using the elastic-plastic model commonly used in practice, the Mohr-Coulomb model. Validation using this model will be followed in phase two with a more advanced model like the hypoplastic model. The validation and material calibration is done on dry medium-dense sand ($R_D=54\%$) and afterwards analysis is performed for loose sand. The second following phase is the validation using an advanced material model such as the hypoplasticity model.

It is shown that with the MPM Mohr-Coulomb material model it is possible to calculate load-displacement curves that closely fit results from the centrifuge tests.

References

Version	Date	Author	Initials	Review	Initials	Approval	Initials
1	Oct. 2013	dr. A. Elkadi		dr.ir. P. Holscher		dr.ir. P.R. Wellens	
		P. Nguyen MSc.					

State
final

Contents

1 Introduction	1
1.1 Goal of this work	1
1.2 Overview of the performed work	1
1.3 Outline of the report	1
2 Overview of the centrifuge experiments	3
2.1 Test set-up	3
2.1.1 Loading system	3
2.1.2 The model pile	3
2.2 Sample properties & preparation	4
2.2.1 Soil properties	4
2.2.2 Sample preparation	5
2.2.3 Description of the tested samples	5
2.2.4 Pile installation	6
2.2.5 Pile testing	6
3 Modelling jacked pile installation in MPM	7
3.1 Geometry, mesh, and boundary conditions	7
3.2 Pile installation procedure in MPM	9
3.2.1 Influence of pile head velocity	9
4 MPM simulations using the Mohr-Coulomb material model	11
4.1 Triaxial results on Baskarp sand and material properties	11
4.2 Mohr-Coulomb parameter calibration	11
4.3 Influence of Young's modulus (E value)	11
4.4 Shaft resistance results from centrifuge experiments	13
4.5 Influence of angle of internal friction	14
4.6 Effect of dilatancy angle	15
4.7 Influence of contact friction coefficient	15
4.8 Influence of stiffness increase with depth	16
4.9 Final fit for Mohr-Coulomb analysis ($R_D=54\%$)	18
4.10 Simulation for the loose sand ($R_D=36\%$)	19
4.11 Conclusions on the validation of pile installation with Mohr-Coulomb model	20
5 Simulation of the Static Load Test (SLT)	21
6 Conclusions and recommendations	25
7 Bibliography	27
 Appendices	
A Triaxial experiment results on Baskarp sand in Deltares (GeoDelft) in 2003	A-1
B Insight into material point stress path near the pile tip	B-1

1 Introduction

1.1 Goal of this work

Goal of the project is to validate calculations using the Material Point Method (MPM code of Deltares) with results of centrifuge experiments on pile installation and static load testing in Baskarp sand.

1.2 Overview of the performed work

Numerical calculations using MPM are performed for the jacked installation of an initially partly embedded pile in dry sand. In the centrifuge tests, three different initial densities of the sand have been investigated (loose, medium-dense, and dense sand). In this work, calculations are performed for two different material parameter sets corresponding to two different densities, namely medium dense and loose sand. The mesh used in this analysis was readily available within the PhD work of Phuong, N. Accordingly, only material model calibration (Mohr-Coulomb) and parameter variation is considered in the current work.

Firstly, Material calibration and parameter variation using the Mohr-Coulomb model is performed for the medium-dense sand to arrive at a parameter set that best fits the experiments. After having completed the analysis of the installation phase with material calibration, an attempt is made to simulate a static pile load test (SLT). The calculation phases of the numerical simulations follow closely the procedure as applied in the centrifuge tests carried out at Deltares under supervision of Paul Hölscher, see Huy (2008) and Hölscher et. al, (2012). Afterwards, simulations are performed using the calibrated material for the loose sand.

1.3 Outline of the report

A short overview is presented on the centrifuge experiments. Then, results of numerical simulations using the Mohr-Coulomb model on medium-dense sand are presented including the parameter variation and final parameter set that best fits the experiments. Afterwards, simulation of the loose sand is performed. Finally, discussion and conclusions on the presented results is given.

2 Overview of the centrifuge experiments

For the validation of the MPM-simulations of pile installation and load tests, results of centrifuge tests carried out at Deltares (Huy, 2008) are available. The centrifuge experiments performed at Deltares are described in detail in Huy (2008) and Hölscher, P., et al. (2012). Hereafter is a summary of the main features of the experimental setup and the performed tests to which the MPM calculations are compared.

2.1 Test set-up

Figure 2.1, shows the test set-up. The tests were carried out in a 0.6 m-diameter and 0.79 m-high steel sand-filled container (sand height 0.46 m). A loading frame with plungers was mounted on top of the container. The model pile was connected to the plungers. The most important components of the set-up are described briefly hereafter.

2.1.1 Loading system

The loading system consisted of two hydraulic actuators (plungers) that were installed in series. The first and largest plunger was fixed on the loading frame, and was used to install the pile in flight to its starting position before the load test programme began. The second, smaller, plunger was the fast loading plunger, and was fixed to the rod of the first plunger. The pile was attached to the second plunger.

2.1.2 The model pile

The model pile was a steel pile with a length of 0.3 m and a diameter of 0.0113 m. The mass of the pile and connector under the load cell at the pile head was 1.08 kg.

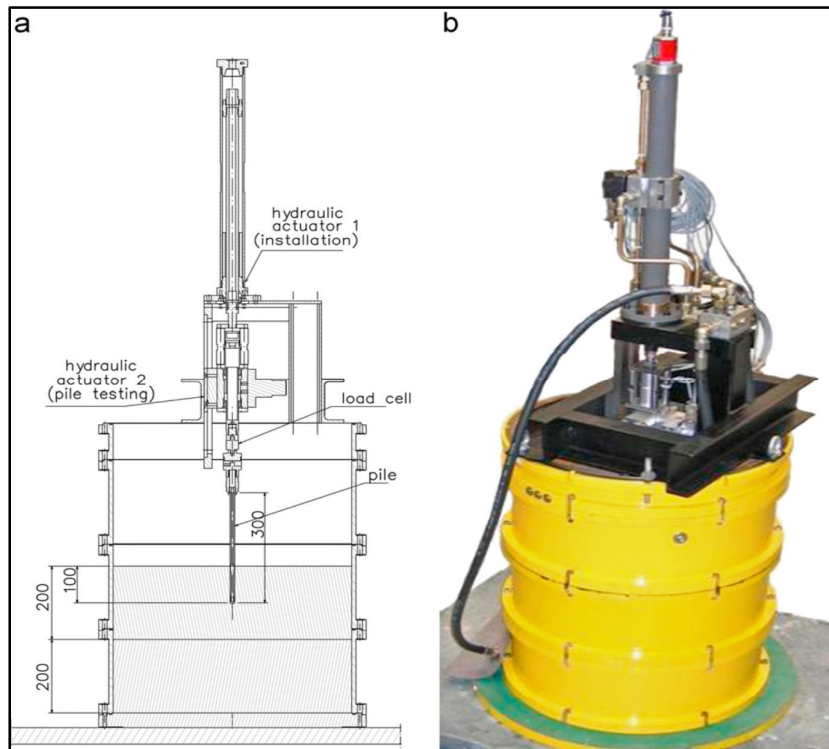


Figure 2.1 Test set-up. a: Dimensions of centrifuge test set-up (the positions of pore water transducers and load cells are shown in Fig. 2), b: Photograph of centrifuge test set-up

A load cell was placed in the model toe to measure pile toe resistance. The pile toe was also equipped with a pore pressure transducer to measure pore pressure directly below the pile toe. For this purpose, a small hole measuring 5 mm in diameter was made to accommodate the transducer.

2.2 Sample properties & preparation

2.2.1 Soil properties

Baskarp sand with a $d_{50}=130\mu\text{m}$ was used for the tests.

Table 2.1 presents the sand's basic properties as determined in laboratory tests, Hölischer, P., et al, (2012). The angle of internal friction is measured using a triaxial test.

Parameter	Value	Dimension
Density of soil particles	2647	kg/m^3
d_{10}	90	μm
d_{50}	130	μm
d_{90}	200	μm
Min. porosity (n_{\min})	34	%
Max. porosity (n_{\max})	46.9	%
Friction angle at $R_D=50\%$ ($n=40\%$)	41	deg.

Table 2.1 Properties of Baskarp sand

2.2.2 Sample preparation

To prepare a homogenous sand body at a pre-determined density, the preparation method described by Van der Poel and Schenkeveld (1998) was applied. This method involves the preparation of water-saturated soil samples with a predefined relative density of between 1% and 2% accuracy.

Where viscous fluid was used, the viscous fluid was carefully positioned above the saturated sand sample. A vacuum was then applied at the bottom of the container and the viscous fluid penetrated into the sand sample. The viscosity of the fluid leaking out at the bottom of the sample was measured; the saturation process was stopped when the measurement equalled the original value of viscosity (Allard and Schenkeveld, 1994).

2.2.3 Description of the tested samples

Only tests 2, 3 and 4 are used for the comparison (after test 1 major changes for improvement of the set-up took place).

The three tests under consideration differ in initial density of the sand sample and the viscosity of the pore fluid.

- Test 2: fine sand, RD=54%, viscous pore fluid (viscosity = 265 cSt*).
- Test 3: fine sand, RD=36%, viscous pore fluid (viscosity = 292 cSt).
- Test 4: coarse sand, RD=65%, water as pore fluid (viscosity =1 cSt).

* 1 unit of dynamic viscosity is centistokes: $1 \text{ cSt} = 1 \text{ mm}^2 \cdot \text{s}^{-1} = 10^{-6} \text{ m}^2 \text{ s}^{-1}$.

2.2.4 Pile installation

During sample preparation, the pile was pre-embedded at a depth of 0.113m, equivalent to 10 times the pile diameter ($10*D$). After the centrifuge had been accelerated, the test began with the installation of the model pile. The first hydraulic actuator pushed the model pile another 0.113m ($10*D$) into the sand bed at a velocity of 10mm/min ($1.67E-04$ m/s). This plunger was then fixed mechanically.

The pre-embedment of $10*D$ was chosen for practical reasons relating to the test set-up. Earlier centrifuge research (Dijkstra, 2009) has shown that after $10*D$ penetration, a steady state is achieved in terms of the stress and the deformation field around the pile toe. The pile may therefore be seen as a soil displacement pile in terms of pile toe behaviour.

2.2.5 Pile testing

The centrifuge tests included a series of axial load tests on a model pile founded in a saturated sand bed (Huy, 2008). During each test, the following variables were measured: displacement of the pile, the force at the head and the toe of the pile, the pore fluid pressure at the pile toe and the pressure in the four buried transducers.

3 Modelling jacked pile installation in MPM

3.1 Geometry, mesh, and boundary conditions

In this report, the installation of the pile into the soil is modelled using the dynamic Material Point Method (MPM) developed and used at Deltares. In MPM, the continuum is represented by Lagrangian points, called material points or particles. Large deformation is modelled by particles moving through an Eulerian fixed mesh. The particles carry all physical properties such as mass, momentum, material parameters, strains, stresses as well as external loads, whereas the Eulerian mesh and its Gauss points carry no permanent information. At the beginning of the time step, information is transferred from particles to the computational mesh. The mesh is then used to determine the incremental solution of the governing equations in a Lagrangian fashion. At the end of the time step, the solution is mapped from the mesh back to particles to update their information.

The model geometry and mesh used in the current work were readily available from the ongoing PhD work of Phoung N. at TU-Delft/Deltares. The following geometry, mesh, boundary conditions are considered:

- A soil wedge of 20 degrees is modelled and by that utilizing symmetry conditions. The pile problem lends itself to axisymmetric condition and by that optimizing in computational cost as compared to full 3D modelling. The mesh discretisation is shown in Figure 3.1.
- For the calculations presented in this report, the side boundary is at a distance from the pile equal to $26*D$ where D is the pile diameter. This is similar to the size of the sample container in the centrifuge experiment.
- The bottom boundary is fixed in x , y , z directions (y : gravity/vertical direction, x,z : horizontal direction).
- The right side boundary is a roller boundary in x direction (normal direction). No use of special boundaries was considered (e.g. absorbing boundaries) due to the large model extent ($26*D$).
- The pile is modelled with rigid body formulation for computational efficiency. Rigid bodies are particularly effective for modelling relatively stiff parts of a model e.g. pile in this case, for which tracking waves and stress distributions are not important. Element stable time increment estimates in the stiff region can result in a very small global time increment. Since rigid bodies and elements that are part of a rigid body do not affect the global time increment, using a rigid body instead of a deformable finite element representation in a stiff region can result in a much larger global time increment, without significantly affecting the overall accuracy of the solution.
- The concept of moving mesh is used where a fixed mesh to the pile can move into the soil. By using this, the fine part of the mesh will always remain around the pile tip (Figure 3.2). For more on the concept of moving mesh in MPM reference is made to Jassim 2013.
- The pile diameter is $D = 0.0113\text{m}$ as in the centrifuge experiments.
- The pile is initially embedded $10*D$ in the soil as described in 2.2.4.
- The number of material points per element is varying in the model for optimizing between computational efficiency and accuracy. 10 material points are used in the area around the pile shaft and pile toe, 20 material points are used in a zone directly under the pile toe, and 4 material points are used for the rest of the mesh (Figure 3.3).

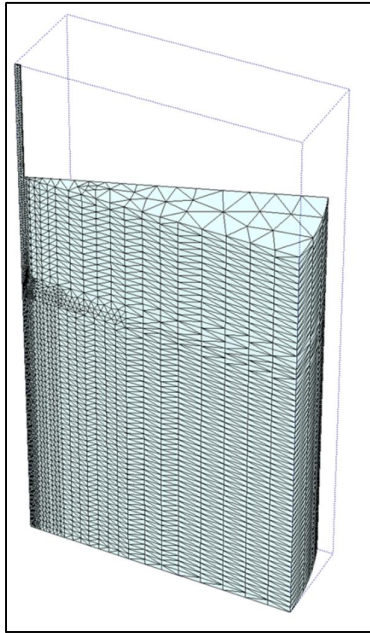


Figure 3.1 Overview of the mesh (pile embedded $10 \cdot D$)

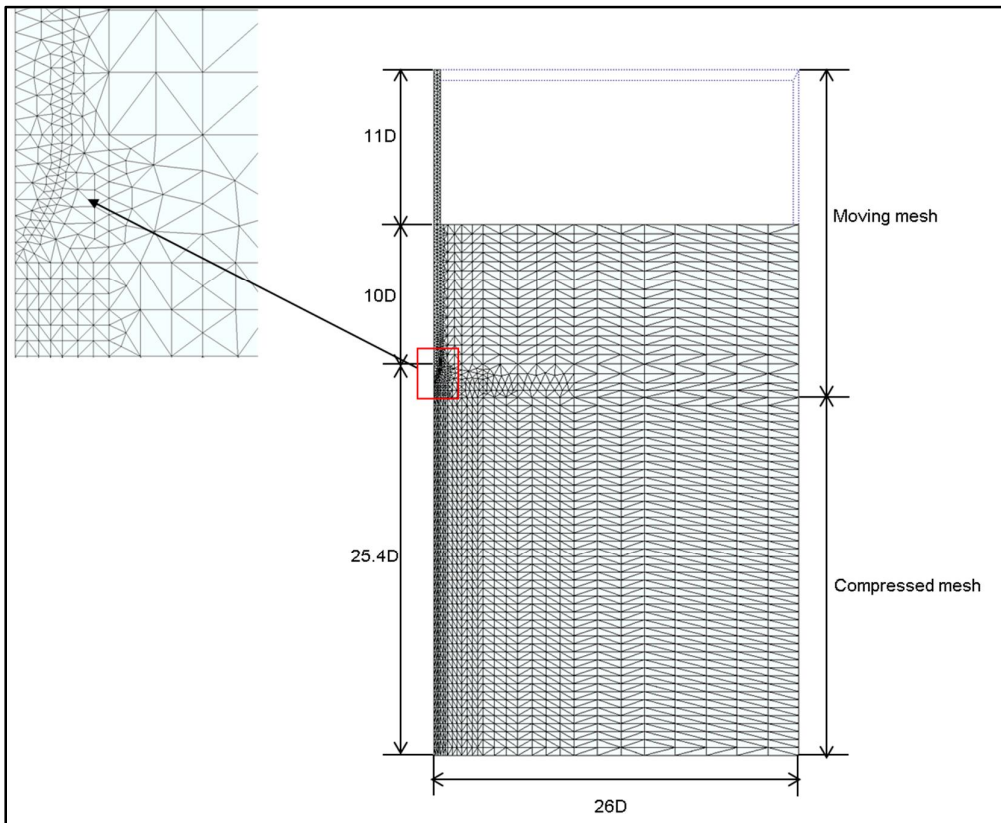


Figure 3.2 Front view of the mesh showing the moving mesh

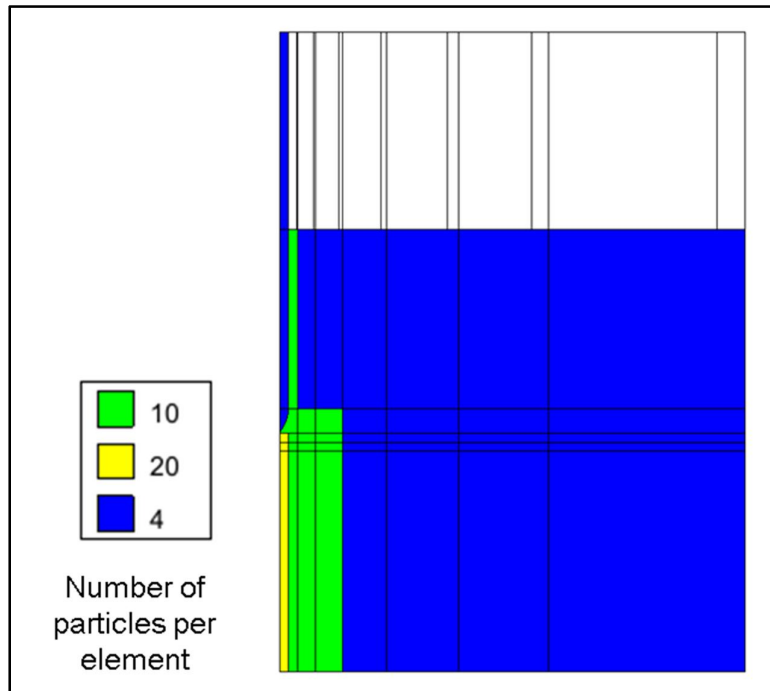


Figure 3.3 Layout of the zoning of material point density as used in different parts of the mesh

3.2 Pile installation procedure in MPM

The following describes the calculation parameters and procedure considered:

- The K_0 -procedure is used to generate the initial stress state ($K_0 = 0.5$) at 1g under quasi-static conditions.
- The initial stress stage (K_0 -procedure) is completed in one load step.
- Afterwards, dynamic analysis is switched on with gravity at 40g to simulate the centrifuge test.
- In the dynamic calculation, an overall local damping factor of 0.15 is chosen. This is the default value advised in the MPM command file description (CPS file) for static penetration problems like CPT and jacked pile installation as in this case.
- A default courant number of 0.98 is used. Value for the Courant number is needed to adjust the time increment Δt based on the size of the critical time step.
- Contact friction coefficient value of 0.176 is used in the contact algorithm to model the frictional behaviour between the pile and the soil.
- Constant surface velocity of 0.02 m/s applied downwards at the pile head boundary is used to simulate the penetration (installation) of the pile in the soil. The effect of head velocity is examined hereafter. Based on this velocity, the installation time of the pile ($10 \cdot D = 0.113\text{m}$) is 5.65 sec.

3.2.1 Influence of pile head velocity

The pile head velocity applied has direct influence on the calculation time. Increasing the velocity, without affecting the accuracy of the analysis, leads to pronounced timesaving in the calculation. However, the velocity used should maintain the static penetration character of the pile installation. Phuong N. compared the behaviour when using a velocity of 0.005m/s and 0.02 m/s on a model with penetration depth till $2 \cdot D$. The result from this analysis is presented

in Figure 3.4. The oscillations with the velocity of 0.02 is larger (please note the horizontal scale is limited to 0.014 kN as compared to 1 kN in the full test) but the overall trend is good.

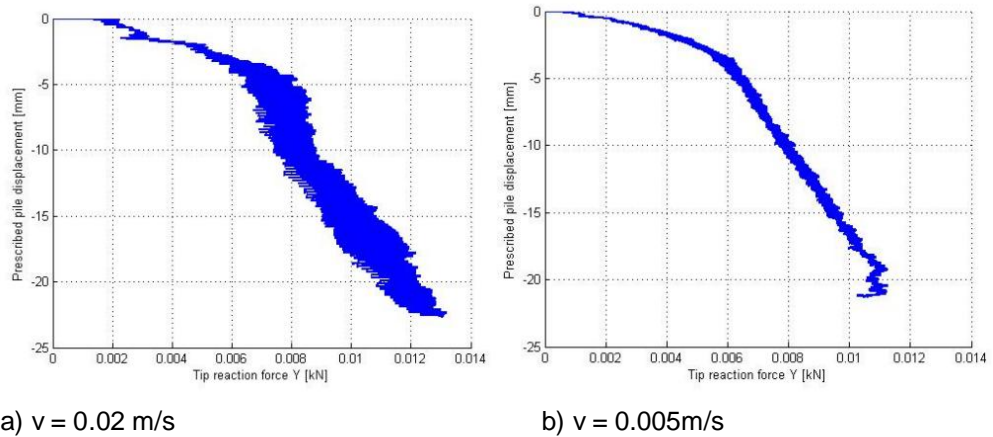


Figure 3.4 Influence of installation velocity on analysis results ($R = 2 \cdot D$)

Further in this work, higher velocities were examined for the full installation of $10 \cdot D$ (Figure 3.5). As seen, the general behaviour is of resemblance but when zooming in, local oscillations increase noticeably with increasing velocity. The result shows that the value 0.02 m/s is rather acceptable is therefore used in the work presented in this report.

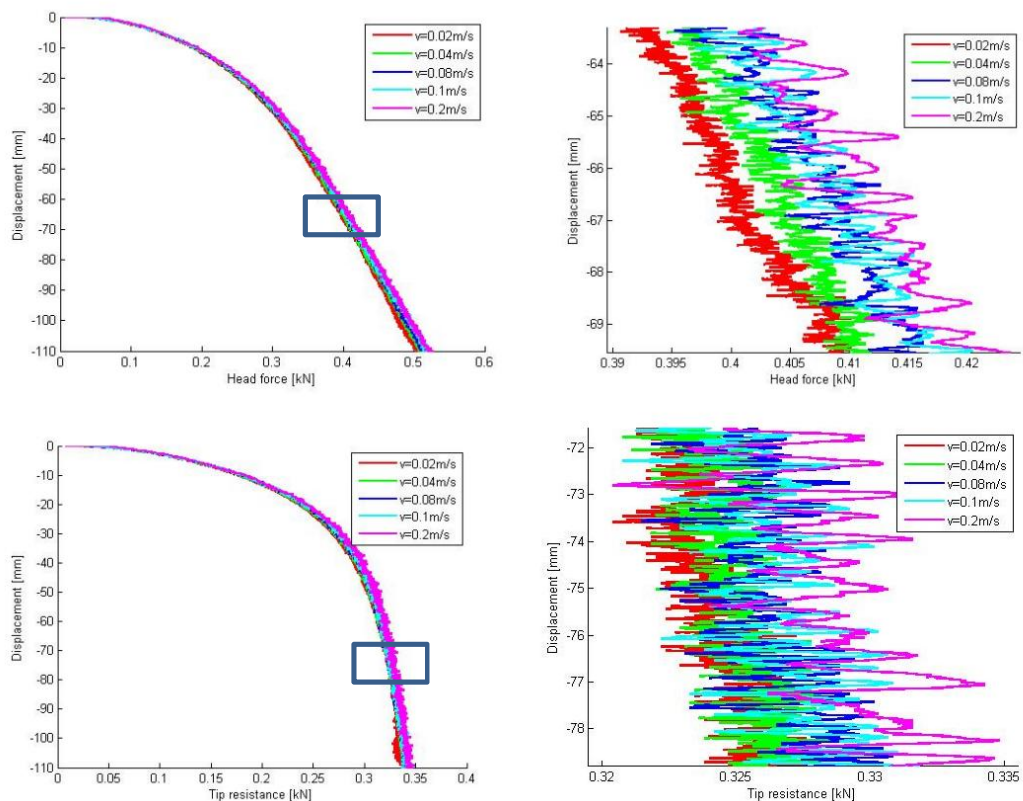


Figure 3.5 Influence of installation velocity on analysis results

4 MPM simulations using the Mohr-Coulomb material model

In this chapter, model simulations of pile installation applying the Mohr-Coulomb model, which is a commonly used model in practice, are presented to simulate the centrifuge tests (Huy, 2010). The parameters used and their influence on the results are given and discussed. A set of material parameters for the Mohr-Coulomb model is chosen as most representative to simulate the centrifuge experiments for medium-dense sand with relative density $R_D=54\%$.

4.1 Triaxial results on Baskarp sand and material properties

In order to obtain a set of parameters to be used in the simulations, results of triaxial laboratory tests on Baskarp sand, conducted at Deltares, are used.

Test results performed in 2003 at Deltares (GeoDelft then) on a sand sample with 40.3% porosity is used. This porosity results in a relative density of nearly 50%, which is close to that of the medium-dense sand in the experiments ($R_D=54\%$).

The triaxial test is performed under a confining pressure of 200kPa, and resulted in the following mechanical parameters:

- Cohesion = 0 kPa.
- Angle of internal friction = 39 deg.
- Dilatancy angle = 15 deg.
- Young's E modulus = 65000 kPa.

4.2 Mohr-Coulomb parameter calibration

For the Mohr-Coulomb analysis in MPM of the centrifuge experiments, the following parameters are selected and examined for best fit:

- Influence of Young's (E) modulus value.
- Influence of angle of internal friction in degrees.
- Influence of dilatancy angle in degrees.
- Influence of friction coefficient in contact algorithm.
- Influence of stiffness dependency with depth.

Further, the following parameters are set for all analyses without variation:

- A value of 1.0kPa is chosen for the apparent cohesion.
- Poisson's ratio=0.3.

4.3 Influence of Young's modulus (E value)

In the classical Mohr-Coulomb, a single value of E modulus is used for the whole soil domain (no stress dependency). In the current analysis, soil is modelled as one layer, as in the experiment, and one value of Young's modulus is assigned for it. The triaxial test results above (4.1) indicate a Young's modulus value of 65 MPa at 200kPa reference pressure.

In Figure 4.1, results of a simulation with $E= 50$ MPa revealed rather good fit with the experiments until a penetration depth of about $1 \cdot D$, which is the initial elastic stiffness region, thereafter the experiments shows a softer response and the simulation overestimates the final force value with nearly 10%. The gradient of the force-displacement curve, however, closely resembles that of the experiment. In this figure, vertically, the pile displacement is plotted,

whereas the calculated/measured force on the pile head and pile tip is plotted horizontally. The value of internal friction angle used here is 30 degrees and dilatancy angle of 0 degrees, which is explained further in section 4.5.

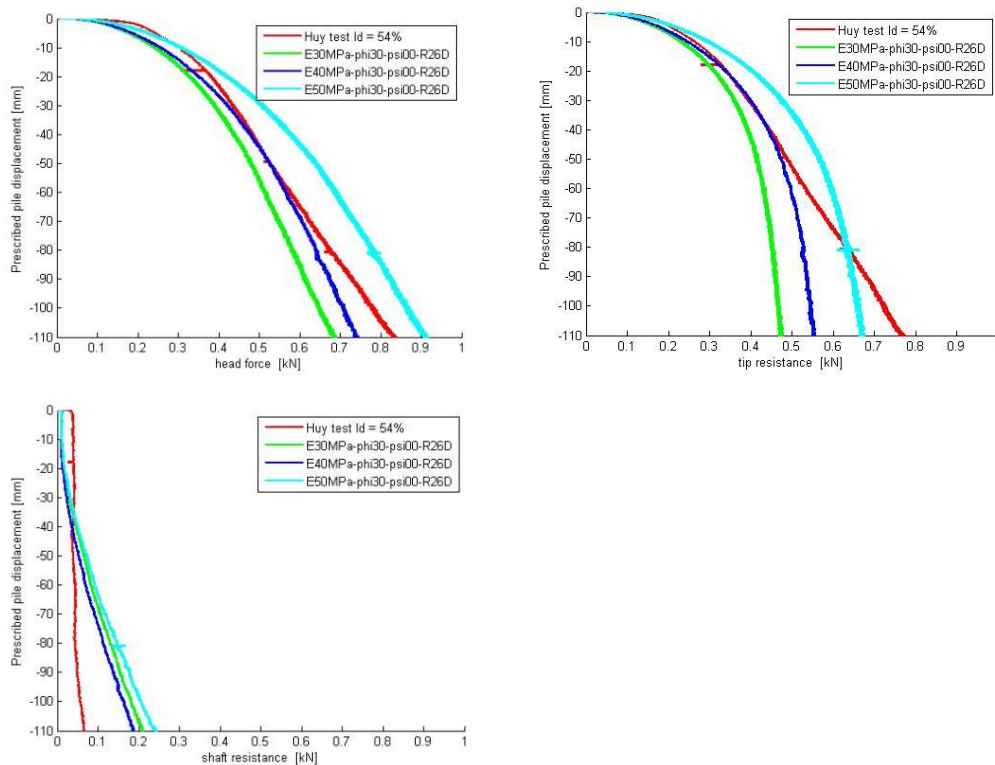


Figure 4.1 Influence of stiffness values in the calculations as compared to the experimental results

Two other values, namely $E=30$ and 40 MPa were examined as well. In Figure 4.1, the results are given of these simulations. In terms of head force, tip, resistance, the analysis with $E=40$ MPa is the most fitting with the experimental results. For the head force, the initial stiffness from the simulation with $E=40$ MPa shows softer behaviour as compared with the experiment but afterwards there is a better match in the depth range of 3^*D-8^*D . Finally, the head force is under-estimated with nearly 10% due to the stiffer behaviour in the experiments. The softer behaviour in the tip result is investigated hereafter.

For the shaft friction, the experiments show a rather constant value with rather slight increase towards the end, which is not reproducible in the simulations. The shaft resistance in the experimental result is calculated as the difference between head-force and tip-force measurements. The tip force measurements are recorded inside the sand sample and are difficult to control/verify, whereas the head-force measurements are usually more accessible. In the next section, it is attempted to examine the validity of tip measurements in the experiments used for validation in this report (Huy, 2008) as compared to other similar experiments done at TU-Delft/Deltares (Chi, 2012 and Dijkstra, 2009).

4.4 Shaft resistance results from centrifuge experiments

The shaft resistance behaviour from three different centrifuge experiments on pile installation (Huy, 2008, Dijkstra, 2009, and Chi, 2012) is examined to assess if the shaft resistance (tip measurements) in the experiments of Huy are representative for use further in this validation. There are differences in these experiments with respect to pile dimensions, etc. but it goes in general over pile installation in sand, which should be good enough for this exercise.

In Figure 4.2, for all tests by Chi, the total shaft resistance starts to increase after 4D penetration. However, in Huy's test, there is only a small increase in the shaft resistance observed after 7D penetration.

In both Chi's and Dijkstra's tests, it is observed that the value of total shaft resistance increases together with the increase of relative density. However in Huy's test, the test of $R_D=36\%$ gives higher shaft friction compared to $R_D=54\%$, which is counterintuitive (Figure 4.3). This gives doubt about the calculated shaft resistance from Huy's test. Based on this, in the remainder of this report focus for validation and comparison is on the head force results. However, the tip results will be displayed as part of the simulation results.

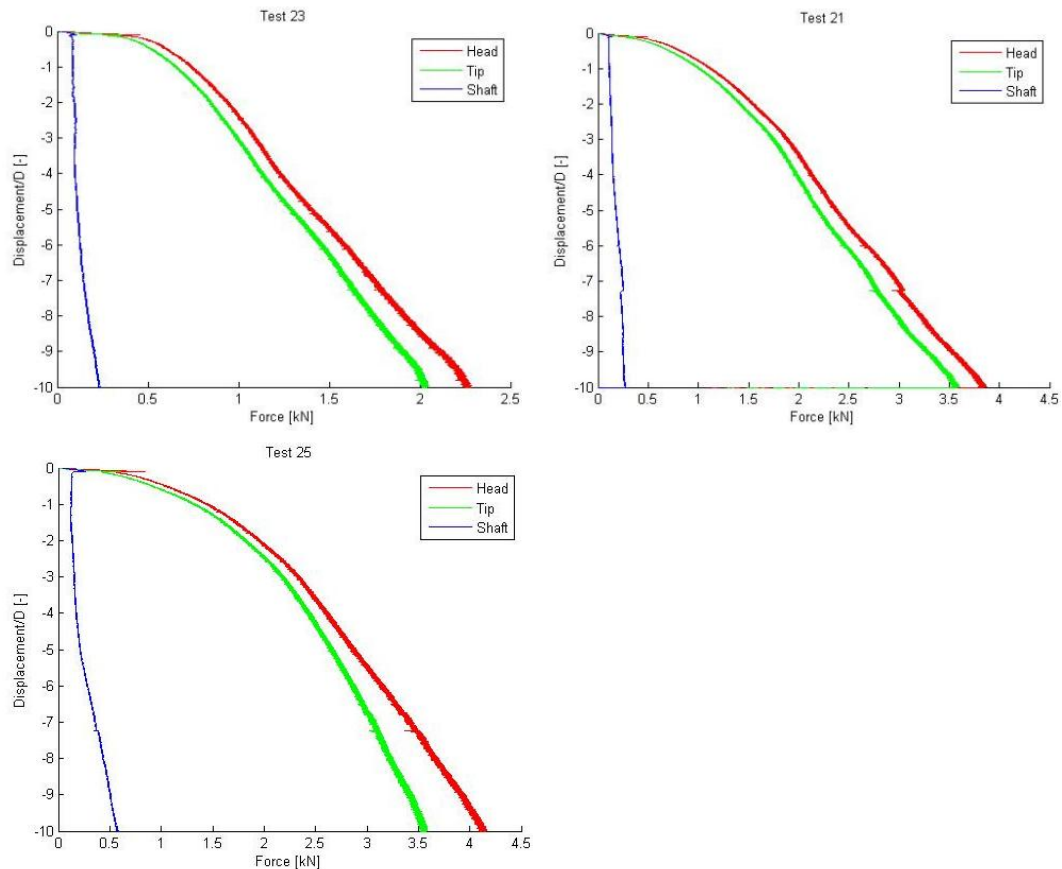


Figure 4.2 Measured force on the pile head, tip, and shaft during pile installation from Chi (2011). Test 23, $R_D=45\%$; test 21: $R_D=65\%$; and test 25: $R_D=65\%$

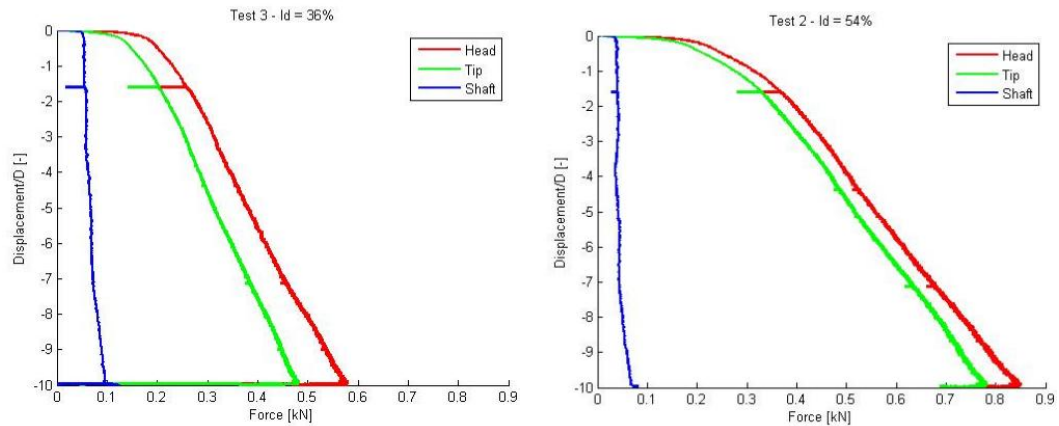


Figure 4.3 Measured force on the pile head, tip, and shaft during pile installation after Huy (2008)

4.5 Influence of angle of internal friction

In Figure 4.4, results are presented of analyses with an angle of internal friction of 39 deg. as from the triaxial test results and with an angle of 30 deg. as calculated hereafter. The analysis with an angle of friction of 30 deg. shows better fit with the experiments in the same way with the Young's modulus since here $E = 40 \text{ MPa}$ is used).

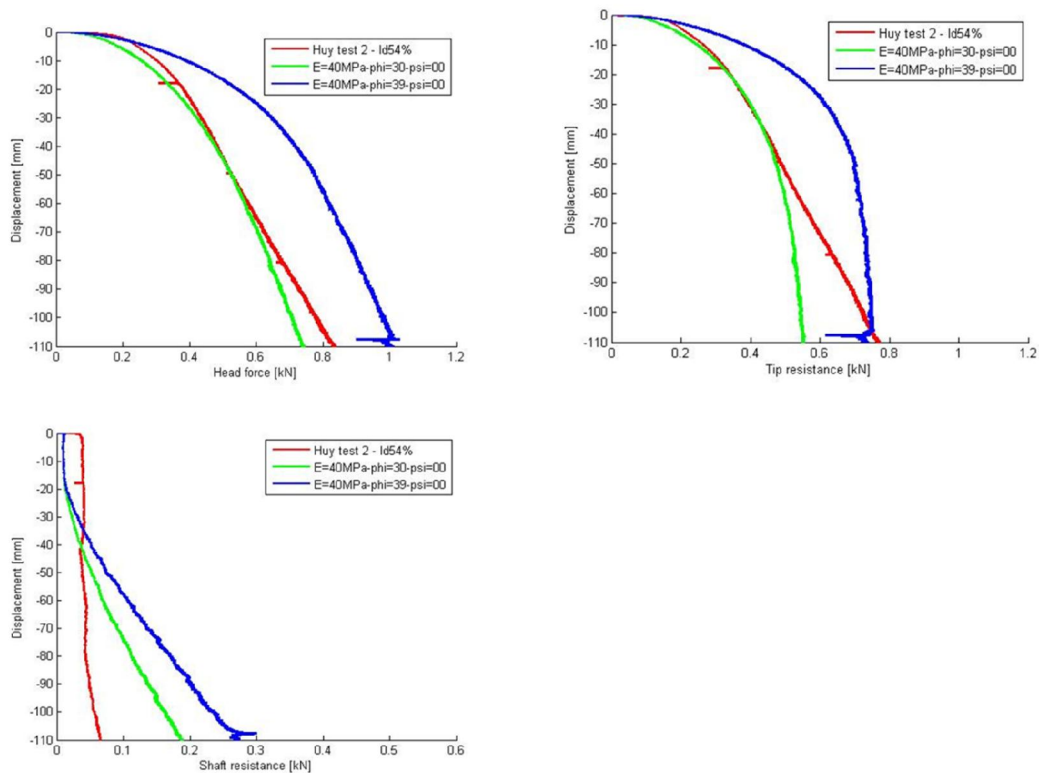


Figure 4.4 Influence of angle of internal friction in the calculations as compared to the experimental results

At the pile tip, the stress values can reach up to 8 MPa or more, which is far larger than the initial stress or the stress level of 200 kPa used in the triaxial experiments. Bolton, M. in 1986 discussed the stress dependency of the angle of friction for sands and presented the following theory to calculate it.

For triaxial compression

$$\varphi'_{\max} - \varphi'_{\text{crit}} = 3I_R$$

The relative dilatancy index I_R is calculated as:

$$I_R = I_D(Q - \ln p') - R$$

In which I_D is the relative density of sand and p' is the applied stress level

For quartz sand (Bolton 1986): $Q=10$, $R=1$, $\varphi'_{\text{crit}}=31$ deg., $p'=8$ MPa and with a relative density of 54%, results in an angle of internal friction of about 30 degree. This is the value used here above.

4.6 Effect of dilatancy angle

It has been attempted to run simulations with varying the dilatancy angle to assess its influence. This was not possible during the project time due to a bug in the code that resulted in failure of analysis attempts for dilatancy angle values > zero. De-bugging and bug fixing attempts took place but a solution is not realized up to the time of writing this report.

However, similar to the stress dependency of the angle of internal friction, Bolton, 1986, discussed stress dependency of the dilatancy angle.

The maximum dilation rate in critical state is (Bolton 1986):

$$\left(-\frac{d\varepsilon_v}{d\varepsilon_1} \right)_{\max} = 0.3I_R$$

Schanz and Vermeer showed that the dilatancy angle could be defined as:

$$\sin \psi = -\frac{\frac{d\varepsilon_v}{d\varepsilon_1}}{2 - \frac{d\varepsilon_v}{d\varepsilon_1}}$$

Which then leads to the form:
$$\sin \psi = \frac{0.3I_R}{2 + 0.3I_R}$$

From this equation and for $p'=8$ MPa, a dilatancy angle of -5.4 deg. is calculated, which indicates contraction rather than dilation near the pile tip. Further from the pile tip and for lower stress levels, the dilatancy could play a role and therefore it remains interesting to check its influence in future work.

4.7 Influence of contact friction coefficient

In literature, the contact angle between steel and sand is advised to be in the order of 17 deg. resulting in a friction coefficient $\mu = \text{TAN}^*17=0.3$. Previous analyses by Phuong, N., 2013, indicated a value of 10 deg. to be of good fit in pile installation modelling with MPM, resulting in a friction coefficient of 0.176.

In Figure 4.5, both values are examined and compared to the experiments and the results show a closer fit with the experiments for a friction coefficient of 0.176. The higher friction coefficient shows a more hardening behaviour with expected overestimation of the head force at the end. As observed in the previous sections with the higher stiffness value and higher angle of internal friction, the gradient of the force-displacement curve at deeper levels shows a better match with the friction coefficient of 0.3, however, the lower friction coefficient of 0.176 matches better in intermediate depths but finally underestimates the total head force.

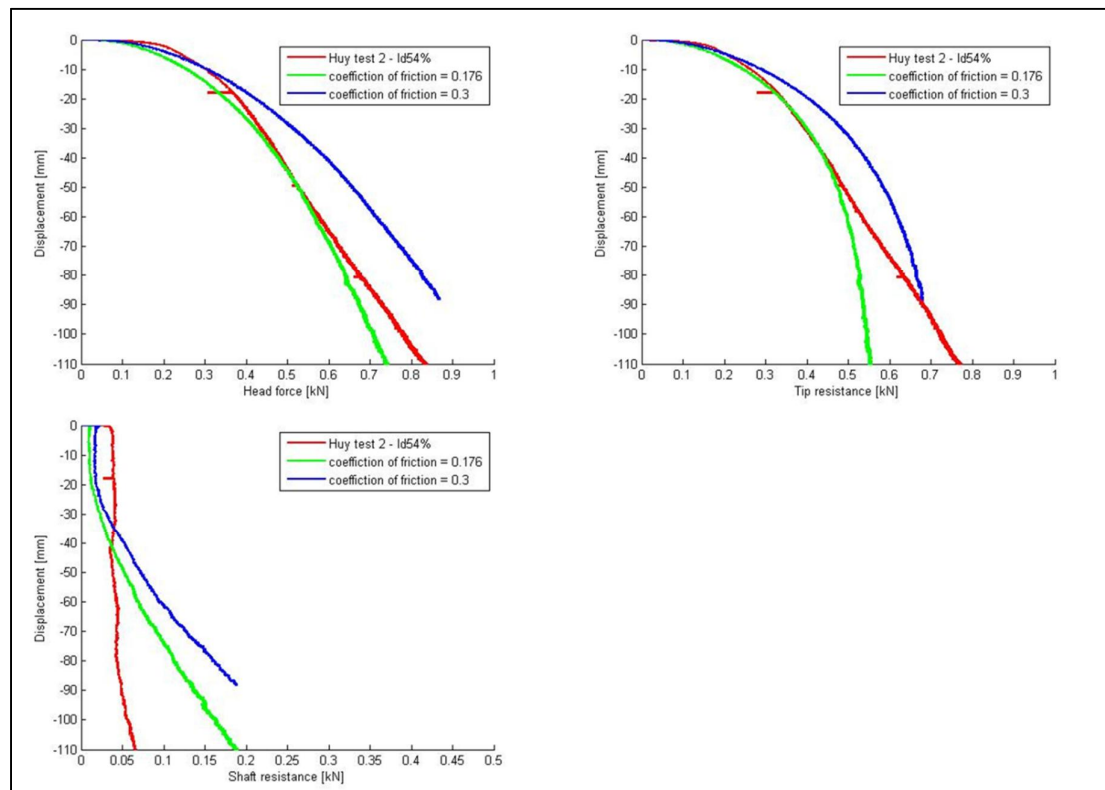


Figure 4.5 Influence of coefficient of friction in contact elements as compared to the experimental results

4.8 Influence of stiffness increase with depth

In the MPM Deltares code, it is possible to increase the shear stiffness (related to Young's modulus through Poisson's ratio using elasticity theory) with depth. Stress dependency of soils with depths is well known.

The increase of shear stiffness with depth takes the form:

$$G = G_0 + \text{Factor} * \text{Depth [per meter]}, \text{ from specified soil surface.}$$

Where G is the shear stiffness related to Young's modulus (E) through: $G = E / 2(1 + \nu)$, with ν is Poisson's ratio.

G_0 is the shear stiffness at a reference level (model surface in this case) = 0 kPa.

The factor used in this calculation is -35700 kPa/m.

In Figure 4.6, the effect of the stress (depth) dependent behaviour of the Mohr-Coulomb model is shown, which indicates a better match with experiments especially in the zone after the friction has been fully mobilised.

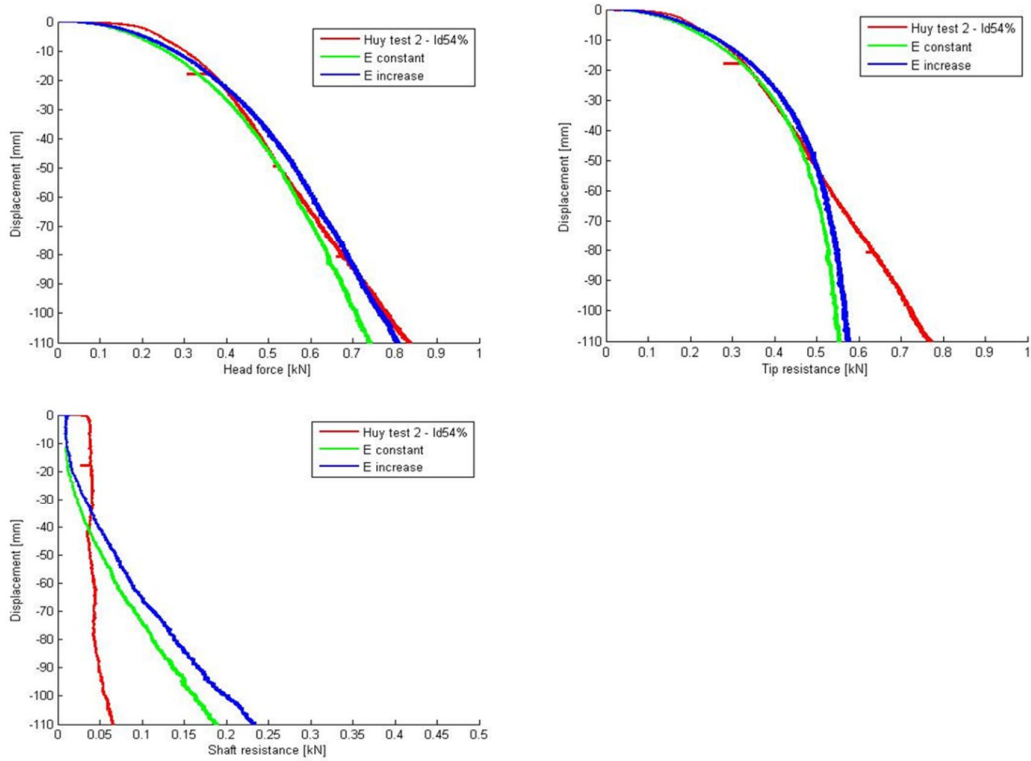


Figure 4.6 Influence of increase of stiffness with depth

4.9 Final fit for Mohr-Coulomb analysis ($R_D=54\%$)

Form the above, a final set of parameters is suggested that best fit the centrifuge experiments of Huy, 2008 on the medium-dense Baskarp sand ($R_D=54\%$). The result of this set as compared to the experiments is given in Figure 4.7. The match with head force is notable. The main good match is the value of the head force together with reasonable fit along the overall force-displacement curve. The final set of parameters is given in Table 4.1.

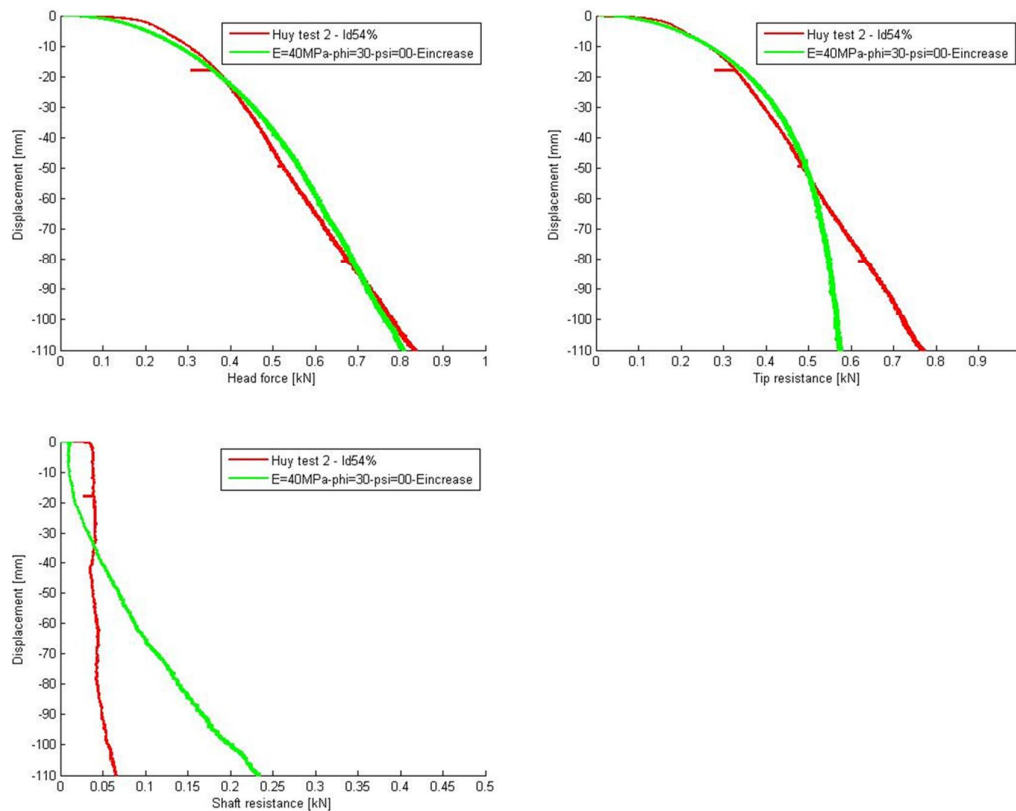


Figure 4.7 final fit for M-C medium dense sand ($R_D=54\%$) as compared with the experiments.

Parameter	Value	Triaxial
Young's modulus (E)	40 MPa	65 MPa
Poisson's ration (ν)	0.3	--
Angle of internal friction (ϕ')	30 degrees.	39 degrees
Dilatancy angle (ψ')	0 degrees	15 degrees
Cohesion (c)	1 kPa.	0 kPa
Increase of shear stiffness with depth	-37500kPa/m	--

Table 4.1 Final set of parameters for Mohr-Coulomb model ($R_D=54\%$)

4.10 Simulation for the loose sand ($R_D=36\%$)

Further to the validation and parameter calibration of for the medium-sand, comparison with loose sand is attempted. The parameters in Table 4.1 are used with only adapting the stiffness value to 25 MPa. The stiffness increase with depth was not included in this analysis. The result is presented in Figure 4.8, which shows a reasonably good fit in terms of overall trend and prediction of the pile's head force. For the loose sand, the measured forces are lower than that of the medium-dense sand resulting in tip stress value of nearly 5MPa. According to Bolton, 1986, as discussed earlier in section 4.5, this stress value results in an angle of internal friction of 29.6 degrees or nearly 30 degrees.

It is observed that in the early penetration depths (initial stiffness) that the numerical result show a softer behaviour as compared to the stiff response in the experiments. The experiments show a sharper transition for the loose sand between the initial stiffness and when tip and shaft resistance start mobilising.

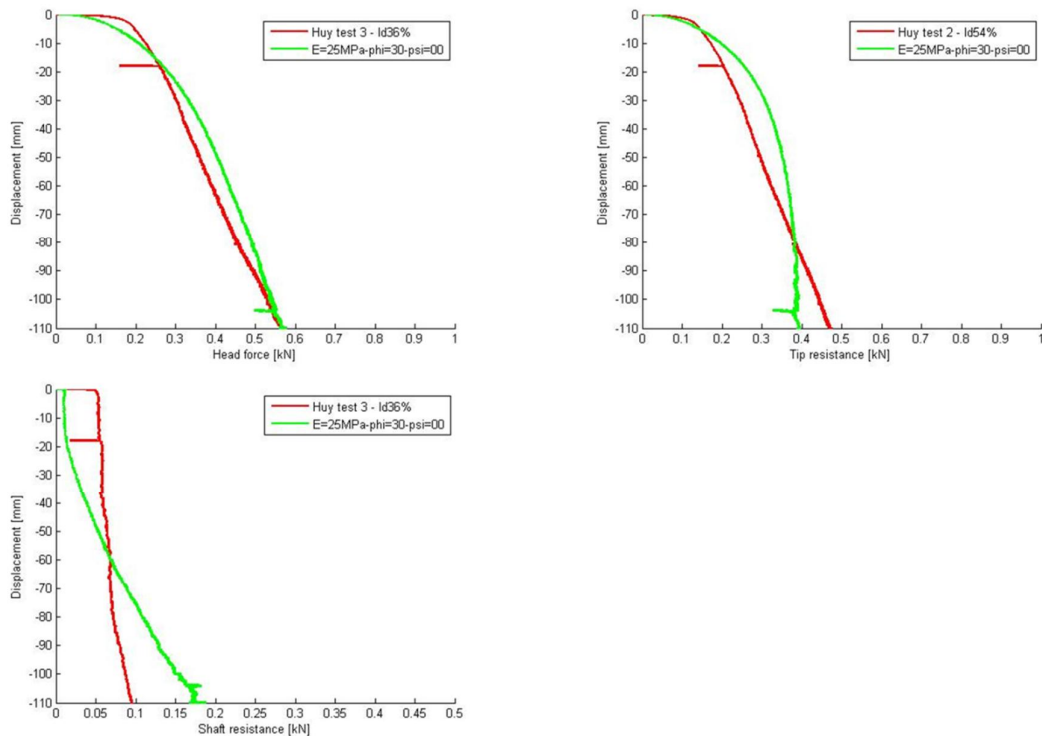


Figure 4.8 Fit for M-C loose dense sand ($R_D=36\%$) as compared with the experiments

4.11 Conclusions on the validation of pile installation with Mohr-Coulomb model

The analysis reported in this chapter, using the Mohr-Coulomb model, shows the capability of the MPM code to simulate pile installation experiments in dry sand in the centrifuge with good fit, especially in terms of pile's head force. Material calibration is needed, however, since parameters from triaxial tests does not immediately provide a good match, mainly due to the different stress levels observed in the pile installation procedure as compared to the ones used in the triaxial test. This calibration could be done using unit element tests and/or well justified correlations in the literature as used in this work (e.g. Bolton 1986 and Schanz and Vermeer 1996).

Further insight into the material behaviour under the pile tip and next to it is gained by closely looking into material point behaviour and their stress-path. This is done for five selected material points and is described in detail in Annex B. It is observed that the material points in the vicinity under the pile tip move vertically along one line under the pressure load of the pile installation. This is after some initial limited lateral slip along the curved conical pile toe. The material points on the side of the pile tip are displaced laterally with the pile advancement. The stress level in the material point under the pile tip increases from less than 100 kPa to nearly 1600 kPa after full pile installation

The analyses were run on PCs with good hardware configuration (e.g. quad-core processors and 16 Gb of RAM) and the analysis time per run was about 4-5 days. This is considering single thread in the simulation due to a bug in parallel processing in MPM.

5 Simulation of the Static Load Test (SLT)

After the simulation of the pile installation, it was continued with the relaxation phase and then the SLT. In the relaxation phase of the centrifuge test, the pile was unloaded to approximately 0kN. In MPM simulation, the relaxation phase was modelled by applied prescribed velocity in the pile head in order to pull the pile upwards to unload it. There are several points that needs attention in this phase as:

- When unloading the pile, the tip resistance or the head force should drop to nearly 0 kN as in the experiment.
- What velocity should be for unloading and reloading the pile?

At this moment, not enough simulations have been done to test the procedure of relaxation phase and SLT, mainly due to a bug in the MPM code when restarting the simulation after installation phase.

Figure 5.2 shows one example of relaxation and SLT phase after pile installation. In this example, the head force is unloaded to nearly 0.1 kN but the tip resistance still stays at 0.3 kN while the shaft resistance is already at -0.2 kN. The ending value of relaxation phase is believed important, as it will influence the load displacement behaviour in SLT. In Figure 5.3, comparison between SLT test in MPM and the experiment is given, which is based on the relaxation phase described here above.

In Figure 5.1, the result of the SLT from centrifuge test shows that the tip resistance, shaft resistance and head force are all starting from more or less the same value of 0 kN.

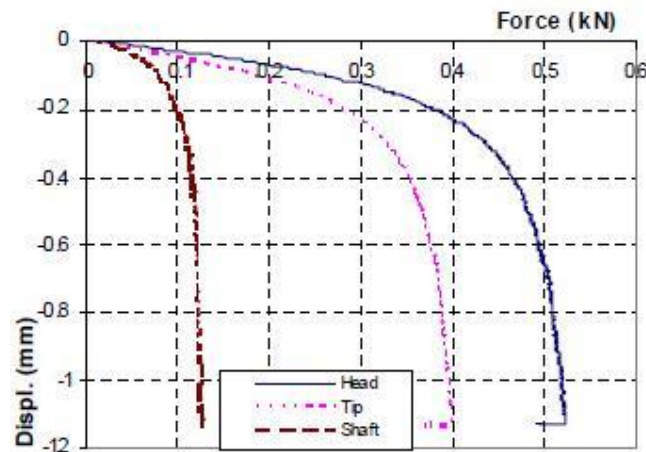


Figure 5.1 SLT result of RD = 54% (after Huy 2008)

Therefore, further work is needed to better simulate the relaxation phase and SLT experiment.

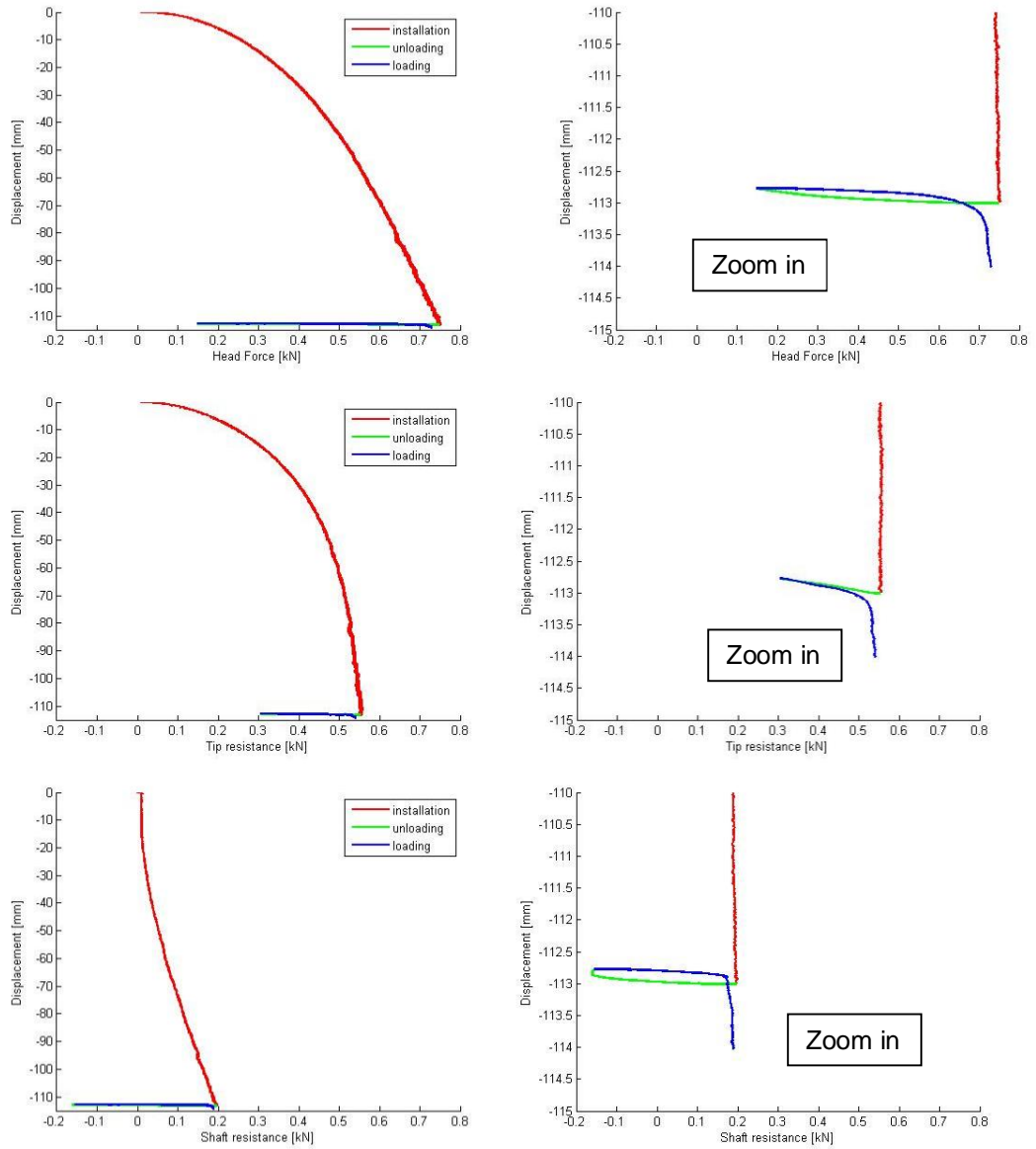


Figure 5.2 Simulation of the relaxation phase in MPM after completion of the installation phase

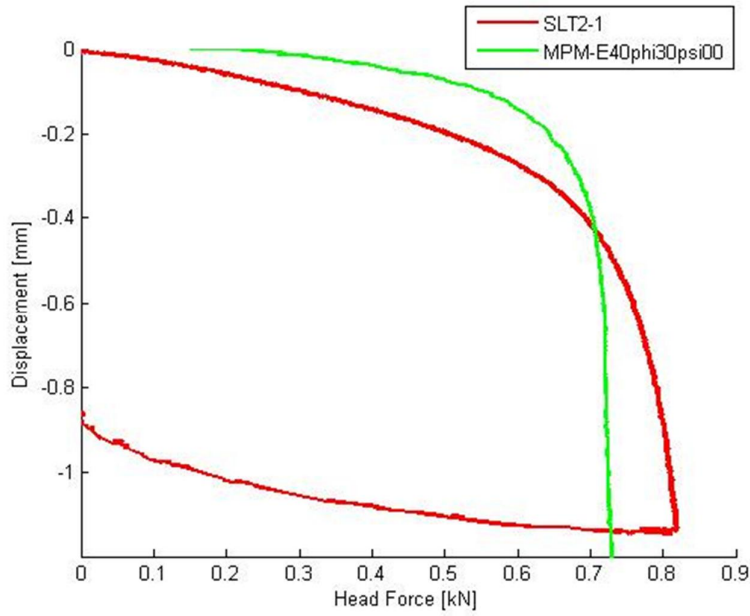


Figure 5.3 Comparison of SLT between MPM and centrifuge experiments (Huy 2008)

6 Conclusions and recommendations

In this report, the progress of the project 1206750-005 is described, during which the jacked installation of displacement pile in the centrifuge experiment is modelled using the MPM code with Mohr-Coulomb material model. First parameter calibration took place for medium-dense Baskarp sand with relative density of 54% to arrive at a parameter set that best matches the experimental results. Afterwards, prediction for the loose sand material was done. Finally, an attempt was made to simulate the Static Load test (SLT). The centrifuge experiments used for validation are from Huy, 2008.

The results as discussed in this report show that the developed MPM-model is capable of predicting load-displacement curves for pile installation in the centrifuge test with good fit. A calibrated parameter set for the Mohr-Coulomb model could reasonably well capture the measured pile head force and overall load-displacement behaviour. When looking more closely there are, however, discrepancies between the simulation and the experiments. This is mainly in the gradient of the descending load-displacement curve. Also, if the initial stiffness is matched, overestimation is reached in the total pile head force, whereas matching the total pile head force and partly the descending load-displacement curve results in a softer initial stiffness.

The results for the tip resistance were not matched due to some doubt in the tip-resistance measurement in the experiments as discussed in section 4.4. The calibration included influence of both strength and deformation parameters of the Mohr-Coulomb model; e.g. Young's modulus, angle of internal friction, contact friction coefficient, and influence of stiffness variation with depth. The influence of dilatancy angle was considered as well but due to a bug in the code, that is being resolved, it was not possible to complete the analysis.

The attempt to simulate the SLT after pile installation indicates the need for more time and bug fixing to be able to better simulate the relaxation phase between the pile installation and SLT.

It is recommended to resolve the bugs related to dilatancy angle, parallel processing, and restart for the future work. It should then be possible to validate further the SLT from the centrifuge experiments.

7 Bibliography

Beuth, L., Vermeer, P.A., Nemeth, A. (2008). Extended quasi-static material point method, Report 35, Institut für Geotechnik der Universität Stuttgart, Germany.

Bolton, M. (1986). The strength and dilatancy of sands. *Geotechnique*, 65-78.

Dijkstra, J. (2009). On the modelling of pile installation. Ph.D. Thesis. Delft University of Technology, Delft, The Netherlands.

Chi, N. (2012). PhD research undergoing. Private communication.

Hölscher, P. et. al. (2012). Rapid pile load tests in the geotechnical centrifuge, *Soils and Foundations*, Vol. 52(6), *December 2012*, 1102-1117

Huy, N.Q. (2008). Rapid Load Testing of Piles in Sand: Effect of Loading Rate and Excess Pore Pressure. Ph.D. Thesis. Delft University of Technology, Delft, The Netherlands.

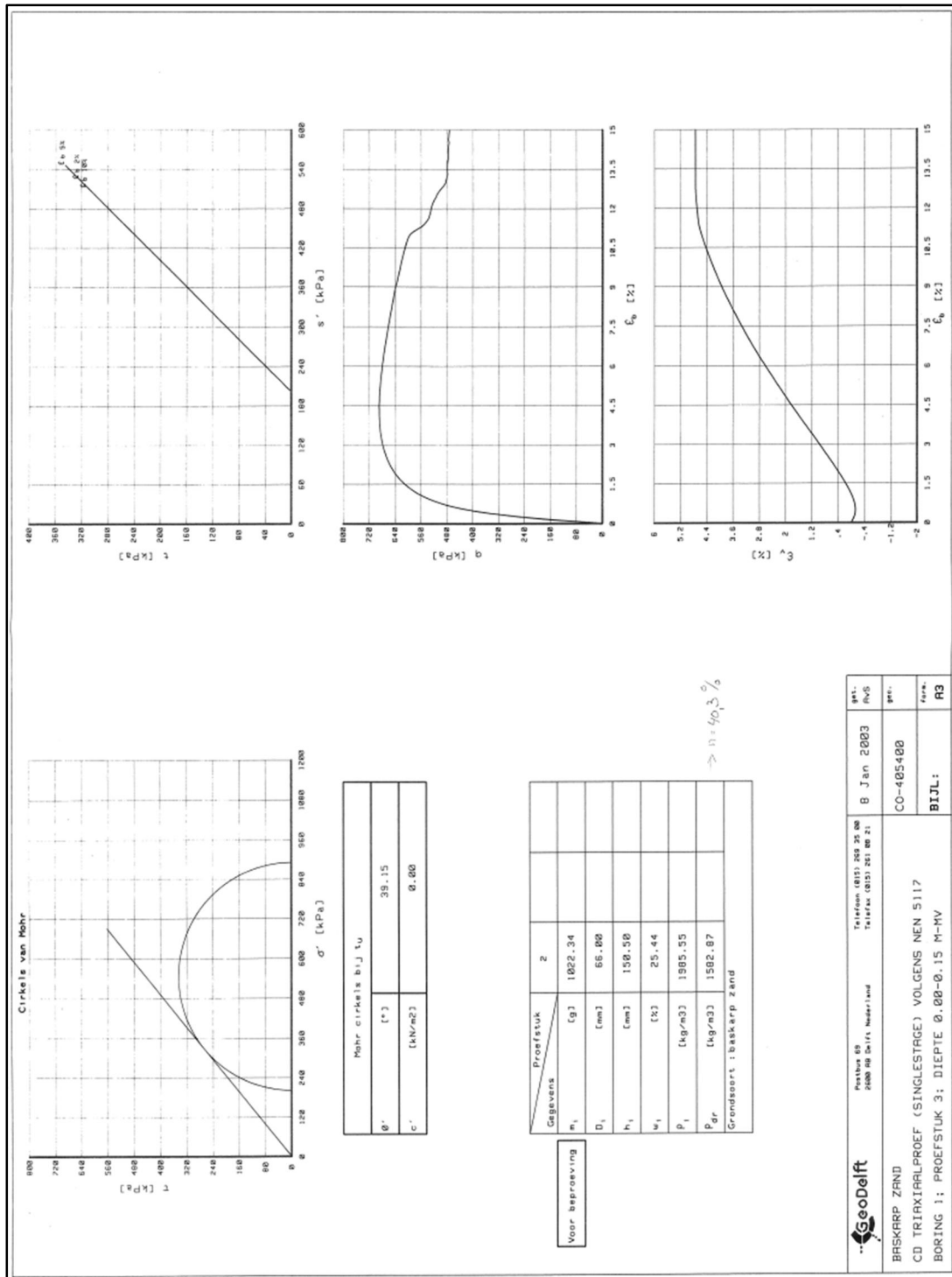
Jassim, I. (2013). Formulation of a Dynamic Material Point Method (MPM), PhD Thesis, Institut für Geotechnik der Universität Stuttgart.

Phuong, N. (2013). PhD research undergoing. Private communication.

Rohe, A., Nguyen, P. (2013). On the validation of the Material Point Method (MPM), Deltares report 1206750-003.

Schanz T., Vermeer P. A. (1996). Angle of friction and dilatancy of sand, *Geotechnique*, Vol.46, No.1.

A Triaxial experiment results on Baskarp sand in Deltares (GeoDelft) in 2003



B Insight into material point stress path near the pile tip

One of the features in the MPM code is the option to trace some material points and to prepare graphs describing the stress path they encounter during the analysis. Five material points are selected under the pile tip and next to it for this purpose (Figure B.7.1). The shaded area in the figure indicates the pile diameter along the horizontal axis and the pile penetration of $10 \cdot D$ along the vertical axis. The initial vertical position of the pile tip is at 0.3 m along the Y-coordinate, whereas the final position after $10 \cdot D$ penetration is at 0.187 m.

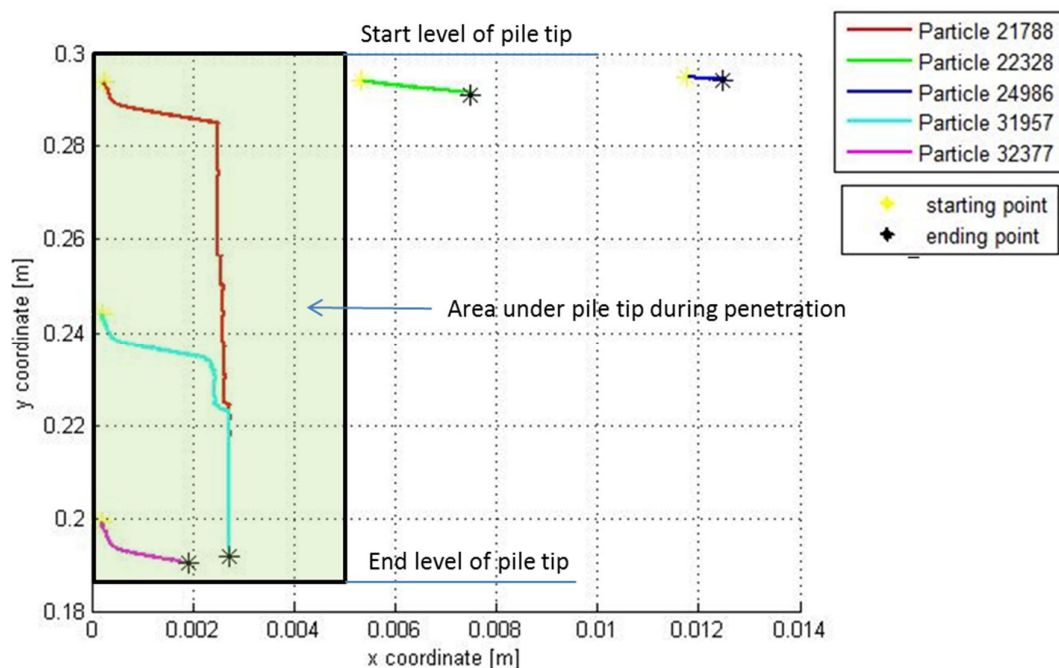


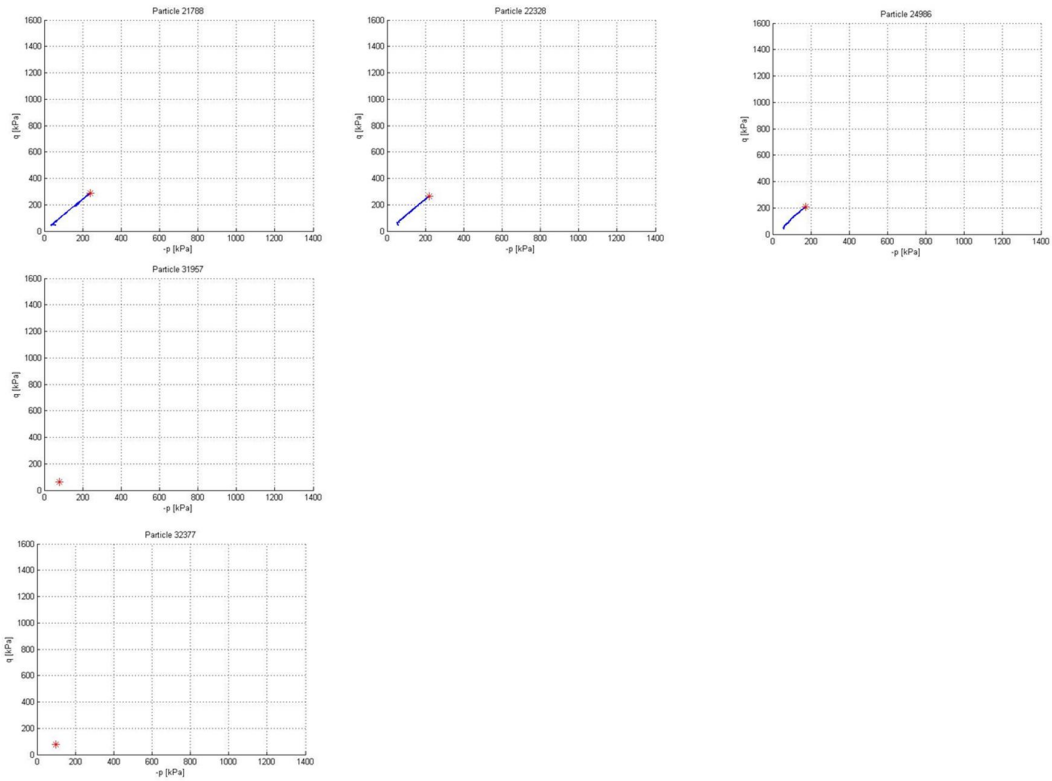
Figure B.7.1 Selected material points and their path during pile installation below and besides the pile tip

It is observed that the material points in the vicinity under the pile tip move vertically along one line under the pressure load of the pile installation. This is after some initial limited lateral slip along the curved conical pile toe. The material points on the side of the pile tip are displaced laterally with the pile advancement.

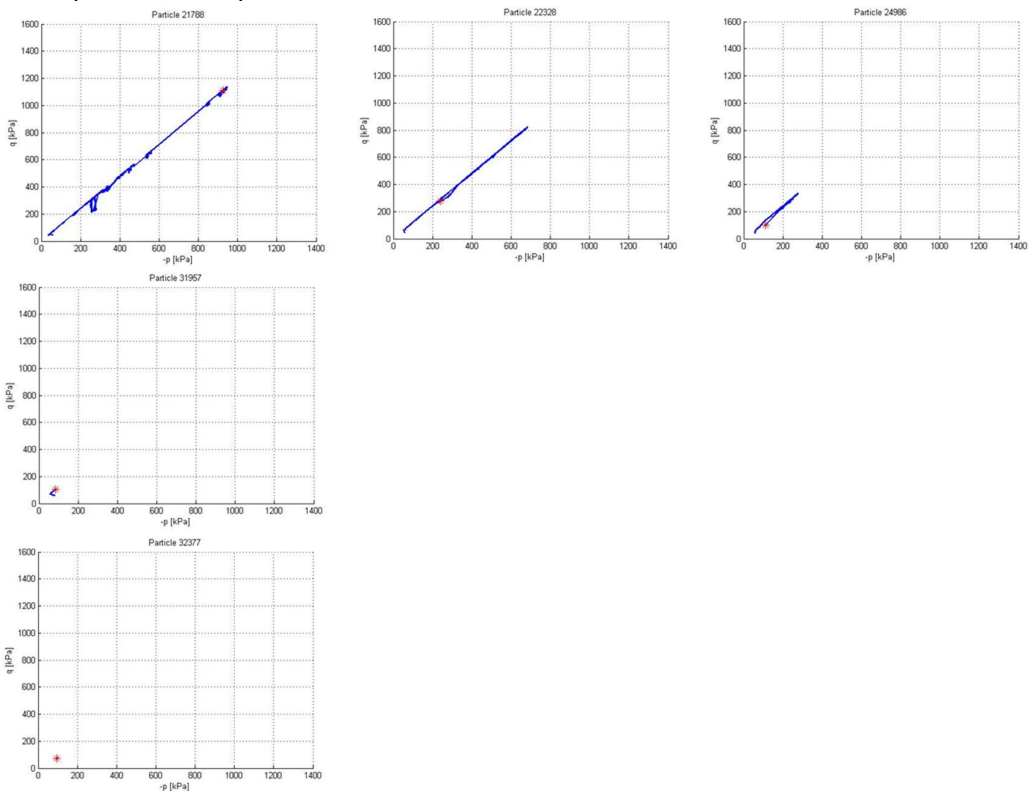
In

Figure B7.2, the stress path graphs for the five selected material points are presented and they show the continuous increase in stress under the pile tip, whereas the material points on the side are initially confined and after the pile penetrates further, they start unloading until more or less their initial stress.

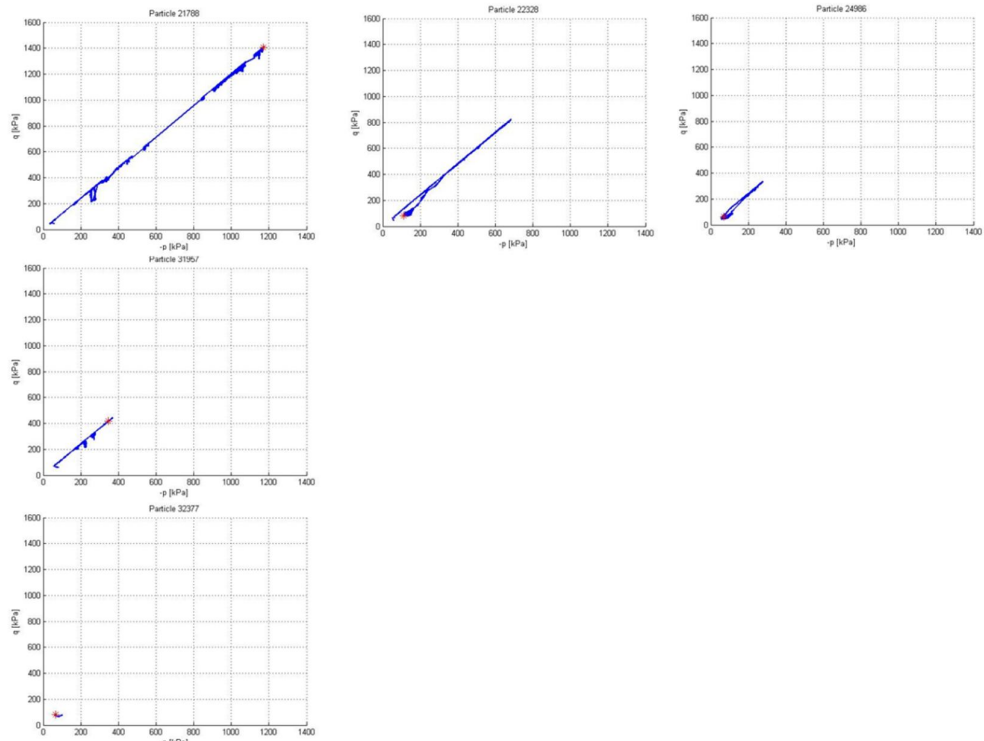
The stress level in the material point under the pile tip increases from less than 100 kPa to nearly 1600 kPa after full pile installation.



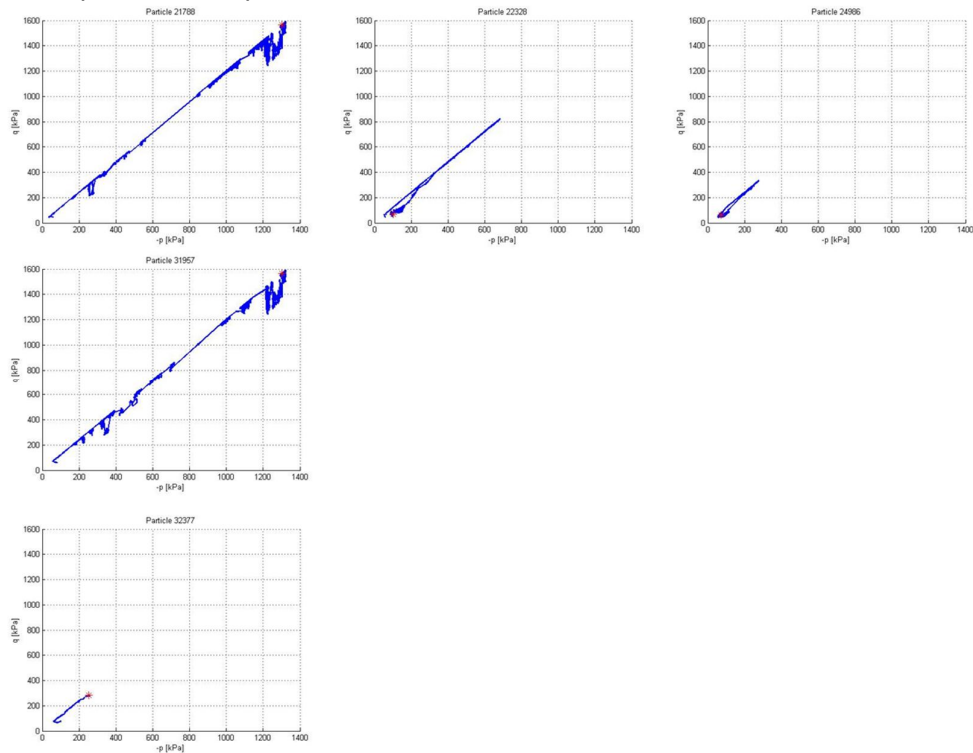
Stress path till 0.5*D penetration



Stress path till 2.0*D penetration



Stress path till 5.0*D penetration



Final stress path till 10.0*D penetration

Figure B7.2 Stress path of five selected material points during different levels of pile installation (0.5, 2, 5, and 10*D)